HHS Public Access

Author manuscript

Exp Eye Res. Author manuscript; available in PMC 2016 December 01.

Published in final edited form as:

Exp Eye Res. 2015 December ; 141: 23–32. doi:10.1016/j.exer.2015.05.012.

Modeling glaucoma in rats by sclerosing aqueous outflow pathways to elevate intraocular pressure

John C. Morrison, **William O. Cepurna**, and **Elaine C. Johnson**

The Kenneth C. Swan Ocular Neurobiology Laboratory, Casey Eye Institute, Oregon Health and Science University

Abstract

Injection of hypertonic saline via episcleral veins toward the limbus in laboratory rats can produce elevated intraocular pressure (IOP) by sclerosis of aqueous humor outflow pathways. This article describes important anatomic characteristics of the rat optic nerve head (ONH) that make it an attractive animal model for human glaucoma, along with the anatomy of rat aqueous humor outflow on which this technique is based. The injection technique itself is also described, with the aid of a supplemental movie, including necessary equipment and specific tips to acquire this skill. Outcomes of a successful injection are presented, including IOP elevation and patterns of optic nerve injury. These concepts are then specifically considered in light of the use of this model to assess potential neuroprotective therapies. Advantages of the hypertonic saline model include a delayed and relatively gradual IOP elevation, likely reproduction of scleral and ONH stresses and strains that may be important in producing axonal injury, and its ability to be applied to any rat (and potentially mouse) strain, leaving the unmanipulated fellow eye as an internal control. Challenges include the demanding surgical skill required by the technique itself, a wide range of IOP response, and mild corneal clouding in some animals. However, meticulous application of the principles detailed in this article and practice will allow most researchers to attain this useful skill for studying cellular events of glaucomatous optic nerve damage.

Keywords

Hypertonic saline; glaucoma; experimental models; intraocular pressure; tonometry; trabecular meshwork; aqueous outflow; optic nerve injury

INTRODUCTION

Intraocular pressure (IOP) is a widely accepted risk factor for glaucoma, and all current glaucoma therapy is directed toward controlling this risk factor. Because not all glaucoma

Corresponding Author: John C. Morrison, M.D., Professor of Ophthalmology, Casey Eye Institute, Oregon Health and Science University, 3181 SW Sam Jackson Park Rd, BRB L467 ADM , Rm 215, Portland OR 97239; phone 503-494-9558, morrisoj@ohsu.edu.

Commercial Disclosures: J.C. Morrison: None, W.O. Cepurna: None, E.C. Johnson: None

patients respond adequately to IOP-lowering treatment, there is still a need to develop novel treatments designed to protect the optic nerve head (ONH) and retina in the face of elevated IOP. Understanding the cellular mechanisms involved in pressure-induced optic nerve damage will greatly facilitate accomplishing this goal.

By the end of the 1980's, the non-human primate glaucoma model, produced either acutely or chronically in monkeys,(Gaasterland and Kupfer, 1974; Quigley and Addicks, 1980; Quigley and Anderson, 1977) was primarily used to study this problem. However, the high cost of animals and their maintenance restricts their use for detailed cell biology studies, since such work requires large numbers of animals to account for individual biologic variability. Because of this, attention has been increasingly directed at the challenge of producing experimental IOP elevation in rodents. Although anatomic differences between the rodent and primate ONH exist, the general plan for this approach was to use the rodent models to understand basic concepts and likely important cell processes. This knowledge could then be used to develop specific hypotheses that could be tested in the primate model, using targeted experiments that test theories of mechanism as well as potential new treatments. This article will first discuss the basic anatomy of the rat ONH, and then describe one of the first-developed rodent glaucoma models--that produced by injection of hypertonic saline into the aqueous humor outflow pathways to produce sclerosis, increased resistance to aqueous humor outflow and elevated IOP.

Anatomy of the rat optic nerve head

Viewed "clinically", from within the eye, the rat ONH is essentially obscured by a striking presence of retinal arteries and veins that may be initially assumed to radiate from the disc. (Figure 1A) However, these vessels actually enter the posterior sclera just inferior to the neural portion of the optic nerve head. This is a fundamental difference from the primate optic nerve, in which the retinal vessels are already within the nerve when they enter the eye. Histologically, in cross section, the neural portion of the rat optic nerve head has an oval shape at the level of Bruch's membrane and sclera, with its short axis oriented vertically. (Figure 1B) This means, when preparing longitundinal sections of the ONH, important for displaying, from anterior to posterior, all layers in a single section, differences in orientation will produce strikingly different appearances. Whereas a horizontal section (Figure 1C) will show the neural tissue adjacent to the sclera and in contact with Bruch's membrane at either edge (similar to what is usually seen in the primate), a vertical section shows a more complex situation (Figure 1D). The neural tissue appears to be narrower at the level of the sclera, representing the short axis of the oval. In addition, the nerve demonstrates intimate contact with the edge of Bruch's membrane only at its superior margin, as the retinal artery and vein, along with other vessels, lie inferior, separating it from the sclera and Bruch's.

Another important feature of the rat ONH lies in the structural composition of the lamina cribrosa. In contrast to the primate, dog, cat, and other larger species, the rat (and mouse) ONH does not have a robust collagenous lamina cribrosa. (Morrison, 1995) While, in the rat, a supportive framework with a basket-like distribution similar to the collagenous lamina is detectable, this is composed almost entirely of astrocytes in association with capillaries.

Since the similarity in their orientation to the collagenous lamina is quite striking, this has been referred to, in both mice and rats, as a “glial lamina”.(Sun et al., 2009) This is appropriate, given that the astrocytes are oriented, as in the primate, across the scleral canal and perpendicular to the axon bundles.(Johnson et al., 2000; Tehrani et al., 2014) In addition to their orientation, the astrocytes are in intimate contact with blood vessels and pial membranes of the ONH. Their nuclei are arranged in columns, similar to those in the anterior portions of the primate ONH.(Anderson, 1969, 1970) Their processes also appear to surround axon bundles, and send numerous, actin-filled processes into the nerve bundles themselves.(Morrison, 2005; Morrison et al., 2011; Tehrani et al., 2014) Ultrastructurally, these processes display intimate contact with individual axons, so that a single axon receives contact from numerous astrocyte processes, and, in turn, each astrocyte likely contacts numerous axons. These considerations indicate that, despite the lack of a collagenous connective tissue component, the glial lamina cribrosa of the rat contains many relationships that will help us use these animals to understand how the cell biology of the ONH responds to increases and fluctuations in IOP and affects axonal damage in human glaucoma.

Posterior to the sclera, the optic nerve gradually assumes a circular shape, primarily through expansion of its vertical dimension. In a group of 8 normal eyes, fixed and embedded in paraffin, the vertical height of the optic nerve at the opening of Bruch’s membrane and 100 μm posterior to this was 85 ± 7 μm (SD) and 95 ± 13 μm, respectively. However, 350 μm posterior to Bruch’s, the width of the neural ONH had approximately tripled to 236 ± 49 μm. This expansion is part of a unique feature of the rodent ONH, termed the “transition zone”. Beginning at the posterior margin of the sclera, the transition zone extends posteriorly until the optic nerve becomes round and fully myelinated, approximately 400 μm posterior to Bruch’s. However, a precise border is difficult to determine as ultrastructural evaluation reveals significant irregularities, with partial myelination of axons, and evidence of astrocytes phagocytosing organelle-containing axonal evulsions, suggesting a degradative pathway that may contribute in some way to glaucomatous axonal degeneration.(Nguyen et al., 2011)

Total axon numbers in the myelinated portion of Brown Norway rat optic nerves have been determined using ultrastructural methods.(Cepurna et al., 2005) Manual counting of all visible axons and extrapolating this to total axons revealed a mean of 121,960 ± 6,680 in 5 month-old animals. Importantly, direct comparisons of right and left eyes in the same animal showed a difference as high as 8.5%. Using this same methodology, total axons in animals aged 24 and 31 months were 123,531 ± 14,326 and 107,231 ± 9,238, respectively. By linear regression, axon counts over all ages showed a statistically significant decrease. However, this was not significant if 31 month old animals were excluded, suggesting that axon numbers begin to show significant reduction only in the last few months of life. This was consistent with the finding that numbers of degenerating axons increased exponentially only in the oldest animals. These results provide important guidance for animal selection, particularly when designing experiments to determine how advanced age might affect pressure-induced optic nerve injury.

Blood supply to the rat optic nerve head

While past debates on mechanisms of axonal injury in glaucoma were once dominated by notions of a “mechanical” vs. “vascular” theory,(Fechtner and Weinreb, 1994; Quigley and Addicks, 1981) these have given way to the concepts of “biomechanical stress/strain” and “ischemia/hypoxia”. Both of these are affected by IOP.(Burgoyne, 2010; Burgoyne et al., 2004) As with the primate, the rat ONH receives blood primarily from the ophthalmic artery. Scanning electron microscopy of plastic castings of microvascular beds has revealed important similarities and differences between the rat and primate ONH blood supply. (Morrison et al., 2005; Morrison et al., 1999; Onda et al., 1995; Sugiyama et al., 1999) In the rat, the ocular blood supply is primarily from the ophthalmic artery, which typically trifucates immediately posterior to the globe, beneath the optic nerve, into two long posterior ciliary arteries and the central retinal artery. The latter, entering the globe inferior to the optic nerve, supplies capillary beds of the retinal nerve fiber layer and anterior portion of the ONH. Capillaries in more posterior portions of the ONH arise from arterioles emanating from the proximal portions of the posterior ciliary arteries, and are continuous with those from the anterior ONH and retrobulbar optic nerve. All of these capillary beds drain into either the central retinal vein, which lies inferiorly, between the nerve and the central retinal artery, or veins that reside within the optic nerve sheath. The optic nerve sheath veins also communicate with the central retinal vein and choroidal veins via a large peripapillary sinus. The presence of this communication highlights the importance of not perturbing any aspect of venous outflow when modeling elevated IOP.

Anatomy of rat aqueous humor outflow

Most experimental models of induced IOP elevation rely on producing increased resistance to aqueous humor outflow. One of these, injection of microbeads into the anterior chamber, is discussed in another article in this Special Issue. Retrograde injection of hypertonic saline relies on the basic anatomy of aqueous humor outflow. In the rat, as in the primate, conventional outflow occurs through the trabecular meshwork, into Schlemm’s canal, and through the limbal sclera via collector channels to the episcleral venous circulation. (Morrison et al., 1995) This episcleral plexus, as well as Schlemm’s canal, is continuous, and can be accessed by retrograde injection into the radially-oriented episcleral veins that drain this plexus. (Figure 2) The hypertonic saline injection technique takes advantage of these relationships to produce scarring of Schlemm’s canal and the trabecular meshwork. (Morrison et al., 1997) It is important to understand that animal species with eyes that lack a continuous Schlemm’s canal, and potentially a limbal plexus as well, may not be good candidates for this procedure.

Animals

The majority of published studies using this model have been performed using Brown Norway rats, although one group has successfully used the Dark Agouti strain.(Cordeiro et al., 2004; Guo et al., 2005) In our hands, Brown Norways are generally docile, requiring, in general, only a brief period of handling in order to obtain reliable awake IOP’s. While in the majority of cases, male retired breeders have been used, this method could readily be adapted to females. Non-pigmented animals are also amenable to hypertonic saline injection,

(Colafrancesco et al., 2011) as the basic anatomy of aqueous humor outflow is similar to that of the Brown Norway. (personal observation) This distinguishes this model from the anterior segment laser method, where the lack of pigment reduces the uptake of laser energy, prompting some investigators to inject India ink or other pigments into the anterior chamber. (Park et al., 2001)

Because most glaucoma occurs in adults, we prefer to use animals that are 6 to 8 months old, or approximately 300 - 400 grams. This is to avoid the potentially confounding influences of a relatively immature visual system that may respond differently to elevated IOP. Should one desire to use younger animals, usually less than 3 months of age, smaller plastic compression rings may be needed for these smaller eyes. No such adaptation is required for animals of advanced age, even up to 28 months.

HYPERTONIC SALINE INJECTION METHOD

The basic challenges of the hypertonic saline injection model are to gain access to one of the radial episcleral veins and confine the injection to the limbus. The instruments required for this procedure are listed in Table 1. This includes manufacturer details for certain instruments, since we have found these to be the most reliable sources for instruments that are of high enough quality to meet the precise demands of this surgical technique.

Details of the microneedle construction and cannulation procedure can be found in published descriptions,(Morrison, 2005; Morrison et al., 1997) but specific points that require emphasis are mentioned here. (see also video, Supplemental Figure 1)

Microneedle: Components and Assembly

The microneedle (Figure 3A -3D) consists of a glass microneedle (3 mm long, measuring 50 – 80 μm outer diameter), polyethylene tubing (Intramedic™ Polyethylene Tubing, PE 50, 427411, Becton, Dickinson and Company, Franklin Lakes, New Jersey, U.S.A.) heated and stretched to a fine taper, and a 23 gauge needle with the point broken off. The microneedle is constructed by heating a 10 μm borosiliacate glass disposable micropipette (VWR, Seattle, WA, USA) with a needle puller and pulling it to the desired thickness. A sample microneedle of proper size used as a reference is helpful, as the needle will have a slight taper, and some portions will be a more appropriate size than others. Using a dissecting microscope, the desired 3 mm needle segment, which will not have a noticeable taper, is cut out with a razor blade. This is inserted into the thin end of the tapered PE tubing (the fit may not be snug), leaving 1.5 – 2 mm of the glass needle outside the tubing. The untapered end of the tubing is then swedged onto the 23 gauge needle, which can then be connected either to a syringe for hand injection or to an injection pump. The joints between the glass microneedle and tubing and tubing and needle are sealed with a small amount of hard-drying epoxy cement (Elmer’s, Columbus, OH, U.S.A.). The glue joint at the needle should ideally be somewhat round, which allows a firm anchor for gripping with the self-closing forceps (Figure 3B), both for beveling (Figure 3C and 3D) and performing the episcleral vein injection. These forceps, (Dumont Self-Closing #N7 Curved Forceps, Fine Science Tools Foster City, CA, USA), should be custom-grooved on their inner, mating surfaces. This provides a “four-point” contact if the round glue joint is grasped, which allows excellent

stability. To sharpen the needle, the forceps are held with a micromanipulator and the needle is gently brought into contact with a rotating, fine-grit aluminum oxide bit mounted on a Dremel tool (Dremel, Racine, WI, U.S.A.) moistened with water, with the needle pointing in the direction of rotation.

Surgical procedure

Animals are anesthetized with an intraperitoneal injection of anesthetic cocktail (ketamine, xylazine and acepromazine) and positioned under an operating microscope with the target vessel pointing toward the limbus, away from the operator. Orienting the animal either to the left or right in relation to the operator will allow easy access to the eye. Given the high magnification required to cannulate these small veins, without extravasation, a foot-drive microscope focus is essential so that both hands can be free to perform the procedure while maintaining sharp focus. The small caliber of the vessel requires that the overlying conjunctiva and connective tissue be incised, so the needle can be precisely inserted. For this, the dissecting scissors and forceps for holding the vessel during cannulation must be as fine as possible. The microneedle, constructed as described above, is attached to a 1 cc syringe.(Morrison et al., 1997) While the investigator can choose a range of saline concentrations, it is essential that this be drawn into the syringe through a 0.22μm filter to prevent particulates from clogging the extremely fine needle.

Because each eye has several radial episcleral veins draining the limbal venous plexus, hyptertonic saline simply injected into one vein is likely to exit an adjacent vein, and not enter the entire limbal plexus, Schlemm's canal or trabecular meshwork. To prevent this, a plastic ring is fitted around the equator of the eye to temporarily block flow in all of the episcleral aqueous veins, except the one being injected. The basic ring has an internal diameter of 5.5 mm, slightly smaller than the globe equator, with an internal groove that allows the ring to fit stably on the equator of the eye. (Figure 3E) A gap is cut in the ring so that when the ring is on the eye, the gap will straddle the vein to be injected, allowing the ring to provide steady compression of the other episcleral vessels against the globe. We typically cast these rings by heat-molding the plastic around a brass mandrel, which is contoured to form the internal dimensions of the ring. The final outer dimensions of the ring are cut on a bench-top metal lathe. In addition to its simplicity, this method allows irregular internal ring features to be produced, which can be used to restrict flow to only portions of the limbal plexus and Schlemm's canal. (Figure 3F) Occasionally, the ring cannot occlude all of the radial vessels. In these cases, vascular microclips, (Figure 3G) ground to a point, can be used to block specific vessels. Instead of the plastic ring, some investigators have made a hole in a rubber glove and pushed the eye into this to achieve constriction of radial episcleral veins. This can be effective, but caution is required to prevent the glove from slipping posterior to the equator, as this may produce less reliable compression of veins and less consistent delivery of saline to the limbus.

In general, episcleral veins suitable for injection can be distinguished from anterior ciliary arteries since the latter are fewer in number, often smaller and supply straight circumferential arteries that do not branch within the limbal plexus. (Figure 2) Often, there are one or more relatively large radial veins on the superior aspect of the globe. The eye can

be rotated down either by an assistant or with a self-retaining speculum that exerts pressure into the inferior fornix. Placing the ring produces an initial blanching of all limbal vessels as the increased pressure forces aqueous out of the eye. As the IOP gradually decreases, episcleral veins become visible as they fill again with blood. After completely dissecting the conjunctiva and all, even fine, connective tissues from the vessel wall, the microneedle is grasped with the curved forceps either on the glue joint or just behind it and brought up to the vessel with the bevel up. Orienting the needle nearly parallel to the vessel improves the chance of cleanly inserting it into the lumen. While grasping only the vessel with the jewelers forceps, the needle is carefully inserted into the vessel just anterior to the forceps. Here the interplay between the two hands is critical. Too much tension with the forceps will pull the vessel too thin to cannulate, while not enough tension will not supply enough counter traction to enable the needle to pierce the vessel wall. Generally, initially relaxing the vessel will allow it to fill slightly with blood and make it easier to engage the vessel wall with the tip of needle. Then, tension is increased slightly while the needle is moved forward and inserted into the lumen, after which the back of the needle may need to be dropped slightly to allow the needle to pass up the vein a short distance without exiting the opposite wall of the vessel.

With the needle in place, an assistant can inject the hypertonic saline either manually or with the aid of a syringe pump. While the pump provides better control of injection force, the variability of microvascular anatomy makes it difficult to control precisely the intravascular pressure at the level of Schlemm's canal. A rough guide to the proper force is that 50 μl should be injected over 10 seconds. Immediate signs that the hypertonic saline has been successfully forced into the angle and across the trabecular meshwork include blanching of the limbal venous plexus and opacity of the lens of the eye. The latter, which is temporary, most likely results from the hyperosmolarity of the saline. Following injection, the needle is removed and the vein occluded with the forceps for 30 seconds. After removal of the plastic ring, the anterior chamber will remain deeper, with posterior concavity of the iris. The supplemental video dynamically illustrates the conjunctival dissection and immediate blanching of limbal vessels from a successful injection. (Supplemental Figure 1) Lack of blanching generally suggests that the likelihood of successful IOP elevation is poor, and almost certainly results from either unsuccessful cannulation or inadequate blockage of a drainage vessel despite the ring and microclips, if used.

As indicated in Table 1, the molarity of the saline can be varied. However, less than 1.5M is unlikely to produce enough scarring to increase IOP. Greater than 2.0M will have an increased risk of inflammation, which can result in ONH and retinal responses that may not reflect the effects of elevated IOP alone.

OUTCOMES OF INJECTION

Intraocular Pressure

Details of measuring IOP tonometrically in rodents are covered in a separate chapter, and both the tonopen(Moore, 1993; Moore et al., 1995) and the TonoLab(Morrison et al., 2009; Pease et al., 2006; Wang et al., 2005) can be used to measure IOP in the rat eye. However, we have identified several factors that will influence these IOP readings, and affect their

usefulness when correlated with optic nerve injury or specific events of the injurious process. These include the use of general anesthetics, which result in unpredictable depression of IOP in both normal and hypertonic saline-treated eyes (Jia et al., 2000a; Wang et al., 2005). The extent of this effect can be as great as 50% of awake IOP. Although it is tempting to calculate an “awake” IOP using this figure, such calculations correlate poorly with actual, awake IOP measurements obtained in the same animals. This is most likely due to the variable effect of anesthesia on individual animals.(Jia et al., 2000a)

Time of day also affects IOP, which demonstrates a distinct circadian rhythm that can only be fully appreciated in awake animals. In the light phase, the IOP in normal eyes measures approximately 20 mmHg by tonopen and TonoLab, while that during the dark is significantly increased to over 30 mmHg. (Kwong et al., 2013; Lozano et al., 2015; Moore et al., 1996; Valderrama et al., 2008) These considerations may apply to mice as well, as Liu has demonstrated higher IOP in the dark in mice monitored telemetrically.(Li and Liu, 2008) However, detailed assessment of this by non-invasive tonometry in awake mice has not yet been performed.

Because higher dark-phase IOP is due to higher rates of aqueous humor formation, (Rowland et al., 1981) and hypertonic saline injection produces increased resistance to aqueous humor outflow,(Morrison et al., 1997) an accentuation of normal circadian fluctuation may occur following saline injection. We have found that, when IOP is monitored in both the dark and light phase, eyes will demonstrate 3 patterns of pressure response.(Jia et al., 2000b) Some show no significant change during either phase, suggesting an inadequate sclerosis of the anterior chamber angle with little effect on outflow resistance. Others demonstrate a significant IOP increase during both the dark and the light phase, consistent with extensive scarring. In the third group, scarring appears to be intermediate, with enough increased outflow resistance to produce a significant IOP elevation only during the dark phase, when aqueous humor production is greatest. The importance of this observation is that eyes that only have IOP elevation in the dark can still demonstrate early optic nerve damage. If IOP measurements are made only during the light phase, the periodic dark phase increases will be missed, resulting in poor correlation of IOP with axonal injury. This phenomenon has also been described in rats using argon laser treatment of the anterior chamber angle,(Kwong et al., 2013) supporting the likelihood that any experimental method that obstructs aqueous humor outflow can produce accentuated dark phase IOP elevation when superimposed on normal circadian variation.

Some investigators attempt to standardize their pressure data by routinely measuring IOP at the same time of day. However, this approach still overlooks the problem of dark phase IOP increases. Instead, for animals housed in light/dark conditions, IOP measurements must be performed during both the light and the dark phase. However, this is time-intensive and requires taking dark-phase readings using lighting restricted to the far-red range of the visible spectrum to avoid influencing circadian IOP rhythms. In addition, the degree of IOP elevation in the dark will still be extensive and correlating pressures to subsequent injury or other analyses will remain difficult. Fortunately, we have determined that, when animals are housed in a constant, low-light level environment (approximately 90 lux), the innate IOP fluctuation is suppressed.(Lozano et al., 2015; Morrison et al., 2005; Pang et al., 2005b) This

maneuver, in addition to reducing one cause of IOP fluctuation, allows the researcher greater latitude on when to measure IOP.

Even with these precautions, though, IOP may fluctuate unpredictably, and awake IOP measurements following hypertonic saline injection, laser and or microbead injection have all been reported capable of reaching peak levels of 50 mmHg, or higher (Fortune et al., 2004; Kwong et al., 2013; Samsel et al., 2010) Measurement at least every other day is necessary to reasonably detect the extent and frequency of these fluctuations.

A successful injection of hypertonic saline will produce scarring of the trabecular meshwork with variable angle closure. (Figure 4A and 4B) This takes several days to develop, and may coincide with recovery of aqueous humor formation, which may be initially depressed from mild, transient inflammation. As a result, IOP in general is initially normal or even low after hypertonic saline injection. (Figure 4C) The extent of IOP elevation can be variable, depending on the degree of angle scarring, although marked early elevation is rare. (Figure 4D)

In our initial report, we noted that, when animals were followed without sacrifice, IOP elevations in some eyes could be sustained for as long as 200 days post injection. Other investigators have followed animals for as long as 4 months(Cordeiro et al., 2004) and in one study reported a mean duration of IOP elevation of 57 days (Guo et al., 2005) In general, though, most investigators will sacrifice animals at a specified time after hypertonic saline injection, since pressures can be variable and longer durations of followup make it more difficult to assemble groups with a uniform pressure response. We generally follow eyes for 5 weeks prior to sacrifice. This represents a reasonable compromise between creating a “chronic” situation and working within parameters suitable for laboratory investigation.

Patterns of axonal injury

A large number of methods exist to assess optic nerve injury, and these are discussed elsewhere in this Special Issue. We have made extensive use of light microscopy to determine the extent of axonal degeneration in cross sections of the myelinated optic nerve. Viewed in this manner, all of the optic nerve axons should be observable in a single section, and small regions or numbers of degenerating axons can be identified. This minimizes the chance that sampling errors due to regional differences in degeneration will result in either over- or underestimates of injury. This is particularly important in glaucoma research, since sectorial injury, likely from regional susceptibility at the level of the ONH, is a characteristic of several models of experimental glaucoma in rodents, as well as human glaucoma.(Dai et al., 2012; Huang and Knighton, 2009; Schlamp et al., 2006)

When viewed in cross-section, degenerating axons can either appear dark without axoplasm, due to collapsed myelin, or swollen, again without axoplasm. Because the latter appearance can also occur if the tissue is allowed to become acutely ischemic, rapid fixation, preferably by perfusion, is important. We have observed that axons degenerate from elevated IOP in our model in a stereotypical pattern, with initial injury appearing in the superior portion of the optic nerve, as shown in Figure 4E.(Morrison et al., 1997) Interestingly, other

investigators, working with laser as well as microbead injection rat models, have also reported superior ONH injury and loss of axons as well as RGCs in the superior retina. (Dai et al., 2012; Huang and Knighton, 2009; Kwong et al., 2013; WoldeMussie et al., 2001) With greater injury, the extent of axonal degeneration appears to spread to other regions of the nerve, with increasing density of degenerating axons and decreasing density of normal appearing axons over the entire nerve cross section. Based on this pattern, we have adopted a qualitative grading scale, rating injury from 1 (no injury) to 5 (degeneration of the entire nerve cross section).(Jia et al., 2000b) A direct comparison of this to manual counts of intact axons by electron microscopy has revealed that each injury grade unit corresponds to a loss of approximately 12,000 axons.(Morrison et al., 2005) Importantly, this analysis also revealed that some eyes with early injury (grade 2) actually had total axon counts that were within the range of normal axon variability.(Cepurna et al., 2005) This means that this injury grading system may be more sensitive to mild injury than counting intact axons, either by light or electron microscopy.

An important caveat with regard to this progression in pattern of injury is that, while one may consider eyes with minimal, focal optic nerve injury or axonal degeneration to be “early”, the variability of IOP response may make it difficult to determine with certainty if this injury progression is clearly what would occur if IOP were truly mild and chronic.

Use of the hypertonic saline model for assessing potential neuroprotective therapies

The hypertonic saline model, as well as other experimental models, offers the opportunity to test potential neuroprotective agents.(Almasieh et al., 2011; Almasieh et al., 2013; Almasieh et al., 2010; Johnson et al., 2014; Pang et al., 2005a) In every trial, in addition to including an untreated or vehicle treated glaucoma model control group, it is essential to measure IOP frequently by methods that minimize the complicating effects of anesthetics and circadian rhythms. As mentioned above, simply measuring IOP at the same time of day for animals housed in typical light/dark environments is not adequate to control for nocturnal IOP peaks. Additionally, each investigator should calibrate their tonometer and validate their technique on cannulated eyes of anesthetized animals.(Moore, 1993; Morrison et al., 2009; Pease et al., 2010; Pease et al., 2006; Wang et al., 2005) Regardless of the glaucoma model, IOP values will vary among animals and with time.

Initially, it must be demonstrated that the IOP histories of the control and treatment group are comparable. For example, in our experience with the hypertonic saline model, IOP measurements need to be made at least three times weekly over the 5 week duration of the experimental period. Less frequent measurements will make it difficult to correlate IOP history with axonal injury. It is especially important to measure IOP at times of peak elevation for the model. In models other than the hypertonic saline model, this may occur within the first hours or day following the experimental procedure.(Fu and Sretavan, 2010; Grozdanic et al., 2003; Kwong et al., 2013; Levkovitch-Verbin et al., 2002; Samsel et al., 2010; Sappington et al., 2009) Early, dramatic peaks in IOP may result in acute injury due to trauma, inflammation and ischemic mechanisms that may or may not be relevant to chronic glaucomatous injury.

Careful analysis as well as documentation of IOP history and its correlation with the degree of optic nerve (or retinal) injury is essential when evaluating neuroprotective agent efficacy. Eyes without detected or minimal IOP elevation should not be eliminated from the analysis, as the lack of injury in these eyes provides confirmation of the accuracy of the IOP history. Regardless of the model, the degree of injury will vary among eyes in the same treatment group. For example, in a recent publication,(Johnson et al., 2014) we found the standard deviation of injury grade to be approximately 1.65 injury grade units (on a scale of 1 to 5, as described above, in Patterns of Axonal Injury). Based on these data and a sample size of 27, we had an 80% power to detect a difference in injury grade of 1.25 units, or an approximately 30% decrease in axon injury. Since neuroprotective strategies are less likely to be effective in the face of high IOPs, one can separately look at injury in those eyes with lower IOP exposure. In this experiment, in a subgroup of 11 eyes with mean IOPs of less than 25 mm Hg, we had sufficient power to detect a similar difference in injury. While no treatment effect was found at either low or high mean IOP in this study, we had ample power to demonstrate that for both treatment groups, lower mean IOPs resulted in significantly less injury. This is a critical point. If the IOP histories are not accurately determined and found comparable, then IOP history differences alone may account for any apparent neuroprotective effect of a treatment.

Regardless of the model used and method of injury assessment, planning for neuroprotective studies should include a statistical determination of sample size for sufficient power, taking into consideration estimations of the variability in IOP history and injury. When determining the effect of treatment, multiple regression analyses can be used to determine the contributions of each relevant parameter, including treatment. Parameters to consider in the analysis of IOP history include mean IOP, peak IOP, duration of IOP elevation and fluctuation in IOP. While integral IOP (area under the curve of IOP vs time) is often used, this must be done with caution, since a high IOP for a short time and a less severe elevation over a longer time frame may produce the same integral IOP but have very different effects on the ONH. Because of these many variables, we believe that collaboration with a statistician, for both planning the experiment and analyzing the data, is highly desirable.

Strengths of hypertonic saline injection for elevating IOP

The hypertonic saline model obstructs aqueous outflow at the anterior chamber angle and trabecular meshwork, the site of outflow obstruction in most forms of human glaucoma. As with the laser and the microbead models, the resulting pressure increase is likely to reproduce stresses in the cornea and sclera that may occur in human glaucoma. More importantly, similar events may also be occurring in the posterior and peripapillary sclera, affording the opportunity to replicate and study biomechanical events that are increasingly being considered to play a major role in glaucomatous axonal injury.(Burgoyne, 2010; Cone-Kimball et al., 2013; Sigal et al., 2011)

In this light, the hypertonic saline injection model should be distinguished from the episcleral cautery model, in which one or more of the large veins that exit the eye beneath the ocular muscles are cauterized or ligated to produce elevated IOP. (Neufeld et al., 1999; Sawada and Neufeld, 1999; Shareef et al., 1995) Direct comparison has demonstrated that

hypertonic saline injection produces anterior chamber deepening, consistent with aqueous humor outflow obstruction, while episcleral vein ligation or cautery does not.(Nissirios et al., 2008) This strongly implies that these two models may also significantly differ with regard to the scleral and peripapillary stresses and strains that their elevated IOP would produce. In addition, the cautery model produces an immediate elevation of IOP. Since the vessels being cauterized may actually be vortex veins, it is likely that this abrupt increase results from obstruction of overall ocular venous outflow.(Morrison et al., 1987) Because these vascular beds are also intimately associated with that of the central retinal vein and optic nerve head,(Morrison et al., 1999) the cautery model may have significant effects on retinal, as well as ONH perfusion that may be very different from those produced solely by obstruction of aqueous humor outflow.

An additional advantage of the hypertonic saline model is that it can be used in virtually any rat or mouse strain, as it does not depend on a specific genetic background or manipulation and the degree of pigmentation should not affect the sclerosis. (Kipfer-Kauer et al., 2010; Walsh et al., 2009) Similarly, all pressure responses are unilateral. This offers the advantage that the fellow, unmanipulated eye can serve as an internal control. Additional advantages of this approach are that the rate of IOP increase following saline injection is relatively slow, and may last for several weeks, or more, and in some eyes tends to increase with time. This slower onset has likely made it easier to detect the pattern of axonal injury progression described above, as opposed to eyes where the IOP is elevated early, sometimes to a high degree, followed by a return to baseline over several weeks.

Challenges of the hypertonic saline model

The major challenge of this technique is the exacting microsurgical skill required to successfully cannulate these small vessels. Excellent visibility requires using a surgical microscope, or a high quality dissecting scope equipped with a foot-drive focus that leaves both hands free to manipulate the vessel and microneedle in a coordinated fashion. Since this also requires high magnification, the surgeons hands must be well supported, which will greatly minimize tremor and improve accuracy. Generally, we have found that with practice these challenges can be overcome and many labs have used this model successfully over the years.(Abdul et al., 2013; Almasieh et al., 2013; Chauhan et al., 2002; Colafrancesco et al., 2011; Cordeiro et al., 2004; Guo et al., 2005; Huang et al., 2007; Prasanna et al., 2005; Taylor et al., 2011; Tezel et al., 2012; Yang et al., 2013)

An additional challenge is to be certain that the ring successfully compresses all radial veins draining the limbal plexus, with the exception of the one being cannulated. When this is not possible, the modified microvascular clips can be highly useful. However, regardless of apparently successful occlusion of all vessels, hypertonic saline injection may still fail to produce an elevated IOP. While this can be overcome with a second injection,(Morrison et al., 1997) our overall experience is that a single injection will produce an IOP elevation in approximately two-thirds of animals. However, some groups report a higher success rate, (Taylor et al., 2011) and all investigators must determine their own rate, so they can allow for enough animals when planning an experiment.

The hypertonic saline model will produce a range of IOP responses.(Fortune et al., 2004) Marked fluctuation can occur with all chronic glaucoma models that employ experimental obstruction of aqueous humor outflow, and models in non-human primates(Kompass et al., 2008; Ollivier et al., 2004) as well as rodents(Levkovitch-Verbin et al., 2005; Pease et al., 2009; Samsel et al., 2010) can all produce peak IOPs ranging as high as 50 and 60 mmHg. However, we generally consider this variability an advantage as it provides opportunities for studying a dynamic range of pressure-induced injury. Careful documentation of IOP produces an excellent correlation between pressure response and injury,(Johnson et al., 2014; Morrison et al., 2005; Pang et al., 2005a; Tehrani et al., 2014) electrophysiology(Almasieh et al., 2010; Chauhan et al., 2002; Fortune et al., 2004) and gene expression responses in the optic nerve head and retina.(Guo et al., 2010; Guo et al., 2011; Johnson et al., 2011; Johnson et al., 2007)

An additional concern is that some eyes can develop significant anterior chamber deepening with corneal enlargement and, in some cases, opacity. However, these changes are not universal, and fundus changes have been documented following this procedure, including alterations in optic nerve appearance by fundus photography and scanning laser ophthalmoscopy, as well as *in vivo* demonstration of RGC apoptosis. (Chauhan et al., 2002; Cordeiro et al., 2004; Morrison et al., 1997)

Summary

The hypertonic saline model relies on the anatomy of aqueous humor outflow to produce scarring of the trabecular meshwork and anterior chamber angle. The resulting outflow obstruction produces IOP elevation that may reproduce corneal, scleral and optic nerve head stresses and strains that are characteristic of human glaucoma. In addition, the onset of IOP elevation tends to be gradual, which may lessen the difficulty of obtaining an accurate IOP history. On the other hand, this method requires fine microsurgical skills and careful attention to detail, and, as with all experimentally-induced models of “chronic” IOP elevation, can result in unpredictable IOP fluctuations. However, with careful planning and documentation of IOP, including a minimum of 3 measurements per week and capturing peak as well as moderate IOPs, excellent correlation of IOP history to nerve damage can be obtained. With these efforts, investigators can successfully use this model to understand mechanisms of pressure-induced optic nerve damage and test potential neuroprotective treatments.

Supplementary Material

Refer to Web version on PubMed Central for supplementary material.

Acknowledgments

Financial Support: NIH grants EY016866, EY010145, 5P30EY010572, Medical Research Foundation of Oregon and an unrestricted grant from Research to 17 Prevent Blindness, Inc.

REFERENCES

Abdul Y, Akhter N, Husain S. Delta-opioid agonist SNC-121 protects retinal ganglion cell function in a chronic ocular hypertensive rat model. Invest Ophthalmol Vis Sci. 2013; 54:1816–1828. [PubMed: 23404122]

Almasieh M, Lieven CJ, Levin LA, Di Polo A. A cell-permeable phosphine-borane complex delays retinal ganglion cell death after axonal injury through activation of the pro-survival extracellular signal-regulated kinases 1/2 pathway. J Neurochem. 2011; 118:1075–1086. [PubMed: 21749374]

Almasieh M, MacIntyre JN, Pouliot M, Casanova C, Vaucher E, Kelly ME, Di Polo A. Acetylcholinesterase inhibition promotes retinal vasoprotection and increases ocular blood flow in experimental glaucoma. Invest Ophthalmol Vis Sci. 2013; 54:3171–3183. [PubMed: 23599333]

Almasieh M, Zhou Y, Kelly ME, Casanova C, Di Polo A. Structural and functional neuroprotection in glaucoma: role of galantamine-mediated activation of muscarinic acetylcholine receptors. Cell death & disease. 2010; 1:e27. [PubMed: 21364635]

Anderson DR. Ultrastructure of human and monkey lamina cribrosa and optic nerve head. Arch Ophthalmol. 1969; 82:800–814. [PubMed: 4982225]

Anderson DR. Ultrastructure of the optic nerve head. Arch Ophthalmol. 1970; 83:63–73. [PubMed: 4983627]

Burgoyne CF. A biomechanical paradigm for axonal insult within the optic nerve head in aging and glaucoma. Exp Eye Res. 2010; 93:120–132. [PubMed: 20849846]

Burgoyne CF, Downs JC, Bellezza AJ, Hart RT. Three-dimensional reconstruction of normal and early glaucoma monkey optic nerve head connective tissues. Invest Ophthalmol Vis Sci. 2004; 45:4388–4399. [PubMed: 15557447]

Cepurna WO, Kayton RJ, Johnson EC, Morrison JC. Age related optic nerve axonal loss in adult Brown Norway rats. Exp Eye Res. 2005; 80:877–884. [PubMed: 15939045]

Chauhan BC, Pan J, Archibald ML, LeVatte TL, Kelly ME, Tremblay F. Effect of intraocular pressure on optic disc topography, electroretinography, and axonal loss in a chronic pressure-induced rat model of optic nerve damage. Invest Ophthalmol Vis Sci. 2002; 43:2969–2976. [PubMed: 12202517]

Colafrancesco V, Coassin M, Rossi S, Aloe L. Effect of eye NGF administration on two animal models of retinal ganglion cells degeneration. Ann. Ist. Super. Sanita. 2011; 47:284–289. [PubMed: 21952154]

Cone-Kimball E, Nguyen C, Oglesby EN, Pease ME, Steinhart MR, Quigley HA. Scleral structural alterations associated with chronic experimental intraocular pressure elevation in mice. Mol Vis. 2013; 19:2023–2039. [PubMed: 24146537]

Cordeiro MF, Guo L, Luong V, Harding G, Wang W, Jones HE, Moss SE, Sillito AM, Fitzke FW. Real-time imaging of single nerve cell apoptosis in retinal neurodegeneration. Proc Natl Acad Sci U S A. 2004; 101:13352–13356. [PubMed: 15340151]

Dai C, Khaw PT, Yin ZQ, Li D, Raisman G, Li Y. Structural basis of glaucoma: the fortified astrocytes of the optic nerve head are the target of raised intraocular pressure. Glia. 2012; 60:13–28. [PubMed: 21948238]

Fechtner RD, Weinreb RN. Mechanisms of optic nerve damage in primary open angle glaucoma. Surv Ophthalmol. 1994; 39:23–42. [PubMed: 7974188]

Fortune B, Bui BV, Morrison JC, Johnson EC, Dong J, Cepurna WO, Jia L, Barber S, Cioffi GA. Selective ganglion cell functional loss in rats with experimental glaucoma. Invest Ophthalmol Vis Sci. 2004; 45:1854–1862. [PubMed: 15161850]

Fu CT, Sretavan D. Laser-induced ocular hypertension in albino CD-1 mice. Invest Ophthalmol Vis Sci. 2010; 51:980–990. [PubMed: 19815738]

Gaasterland D, Kupfer C. Experimental glaucoma in the rhesus monkey. Invest Ophthalmol. 1974; 13:455–457. [PubMed: 4208801]

Grozdanic SD, Betts DM, Sakaguchi DS, Allbaugh RA, Kwon YH, Kardon RH. Laser-induced mouse model of chronic ocular hypertension. Invest Ophthalmol Vis Sci. 2003; 44:4337–4346. [PubMed: 14507878]

Guo L, Moss SE, Alexander RA, Ali RR, Fitzke FW, Cordeiro MF. Retinal ganglion cell apoptosis in glaucoma is related to intraocular pressure and IOP-induced effects on extracellular matrix. Invest Ophthalmol Vis Sci. 2005; 46:175–182. [PubMed: 15623771]

Guo Y, Cepurna WO, Dyck JA, Doser TA, Johnson EC, Morrison JC. Retinal cell responses to elevated intraocular pressure: a gene array comparison between the whole retina and retinal ganglion cell layer. Invest Ophthalmol Vis Sci. 2010; 51:3003–3018. [PubMed: 20071680]

Guo Y, Johnson EC, Cepurna WO, Dyck JA, Doser T, Morrison JC. Early gene expression changes in the retinal ganglion cell layer of a rat glaucoma model. Invest Ophthalmol Vis Sci. 2011; 52:1460–1473. [PubMed: 21051717]

Huang W, Fileta JB, Filippopoulos T, Ray A, Dobberfuhl A, Grosskreutz CL. Hsp27 phosphorylation in experimental glaucoma. Invest Ophthalmol Vis Sci. 2007; 48:4129–4135. [PubMed: 17724197]

Huang XR, Knighton RW. Altered F-actin distribution in retinal nerve fiber layer of a rat model of glaucoma. Exp Eye Res. 2009; 88:1107–1114. [PubMed: 19450448]

Jia L, Cepurna WO, Johnson EC, Morrison JC. Effect of general anesthetics on IOP in rats with experimental aqueous outflow obstruction. Invest Ophthalmol Vis Sci. 2000a; 41:3415–3419. [PubMed: 11006233]

Jia L, Cepurna WO, Johnson EC, Morrison JC. Patterns of intraocular pressure elevation after aqueous humor outflow obstruction in rats. Invest Ophthalmol Vis Sci. 2000b; 41:1380–1385. [PubMed: 10798653]

Johnson EC, Cepurna WO, Choi D, Choe TE, Morrison JC. Radiation Pretreatment Does Not Protect the Rat Optic Nerve From Elevated Intraocular Pressure-Induced Injury. Invest Ophthalmol Vis Sci. 2014

Johnson EC, Deppmeier LM, Wentzien SK, Hsu I, Morrison JC. Chronology of optic nerve head and retinal responses to elevated intraocular pressure. Invest Ophthalmol Vis Sci. 2000; 41:431–442. [PubMed: 10670473]

Johnson EC, Doser TA, Cepurna WO, Dyck JA, Jia L, Guo Y, Lambert WS, Morrison JC. Cell proliferation and interleukin-6-type cytokine signaling are implicated by gene expression responses in early optic nerve head injury in rat glaucoma. Invest Ophthalmol Vis Sci. 2011; 52:504–518. [PubMed: 20847120]

Johnson EC, Jia L, Cepurna WO, Doser TA, Morrison JC. Global changes in optic nerve head gene expression after exposure to elevated intraocular pressure in a rat glaucoma model. Invest Ophthalmol Vis Sci. 2007; 48:3161–3177. [PubMed: 17591886]

Kipfer-Kauer A, McKinnon SJ, Frueh BE, Goldblum D. Distribution of amyloid precursor protein and amyloid-beta in ocular hypertensive C57BL/6 mouse eyes. Curr Eye Res. 2010; 35:828–834. [PubMed: 20795865]

Kompass KS, Agapova OA, Li W, Kaufman PL, Rasmussen CA, Hernandez MR. Bioinformatic and statistical analysis of the optic nerve head in a primate model of ocular hypertension. BMC Neurosci. 2008; 9:93. [PubMed: 18822132]

Kwong JM, Vo N, Quan A, Nam M, Kyung H, Yu F, Piri N, Caprioli J. The dark phase intraocular pressure elevation and retinal ganglion cell degeneration in a rat model of experimental glaucoma. Exp Eye Res. 2013; 112:21–28. [PubMed: 23603611]

Levkovitch-Verbin H, Quigley HA, Martin KR, Harizman N, Valenta DF, Pease ME, Melamed S. The transcription factor c-jun is activated in retinal ganglion cells in experimental rat glaucoma. Exp Eye Res. 2005; 80:663–670. [PubMed: 15862173]

Levkovitch-Verbin H, Quigley HA, Martin KR, Valenta D, Baumrind LA, Pease ME. Translimbal laser photocoagulation to the trabecular meshwork as a model of glaucoma in rats. Invest Ophthalmol Vis Sci. 2002; 43:402–410. [PubMed: 11818384]

Li R, Liu JH. Telemetric monitoring of 24 h intraocular pressure in conscious and freely moving C57BL/6J and CBA/CaJ mice. Mol Vis. 2008; 14:745–749. [PubMed: 18431454]

Lozano DC, Hartwick AT, Twa MD. Circadian rhythm of intraocular pressure in the adult rat. Chronobiol. Int. 2015:1–11.

Moore CG, Epley D, Milne ST, Morrison JC. Long-term non-invasive measurement of intraocular pressure in the rat eye. Curr Eye Res. 1995; 14:711–717. [PubMed: 8529407]

Moore CG, Johnson EC, Morrison JC. Circadian rhythm of intraocular pressure in the rat. Curr Eye Res. 1996; 15:185–191. [PubMed: 8670727]

Moore CG, Milne ST, Morrison JC. Noninvasive measurement of rat intraocular pressure with the Tono-Pen. Invest Ophthalmol Vis Sci. 1993; 34:363–369. [PubMed: 8440590]

Morrison J, Farrell S, Johnson E, Deppmeier L, Moore CG, Grossmann E. Structure and composition of the rodent lamina cribrosa. Exp Eye Res. 1995; 60:127–135. [PubMed: 7781741]

Morrison JC. Elevated intraocular pressure and optic nerve injury models in the rat. J Glaucoma. 2005; 14:315–317. [PubMed: 15990616]

Morrison JC, Cepurna Ying Guo WO, Johnson EC. Pathophysiology of human glaucomatous optic nerve damage: insights from rodent models of glaucoma. Exp Eye Res. 2011; 93:156–164. [PubMed: 20708000]

Morrison JC, DeFrank MP, Van Buskirk EM. Comparative microvascular anatomy of mammalian ciliary processes. Invest Ophthalmol Vis Sci. 1987; 28:1325–1340. [PubMed: 3610551]

Morrison JC, Fraunfelder FW, Milne ST, Moore CG. Limbal microvasculature of the rat eye. Invest Ophthalmol Vis Sci. 1995; 36:751–756. [PubMed: 7890506]

Morrison JC, Jia L, Cepurna W, Guo Y, Johnson E. Reliability and sensitivity of the TonoLab rebound tonometer in awake Brown Norway rats. Invest Ophthalmol Vis Sci. 2009; 50:2802–2808. [PubMed: 19324849]

Morrison JC, Johnson EC, Cepurna W, Jia L. Understanding mechanisms of pressure-induced optic nerve damage. Prog Retin Eye Res. 2005; 24:217–240. [PubMed: 15610974]

Morrison JC, Johnson EC, Cepurna WO, Funk RH. Microvasculature of the rat optic nerve head. Invest Ophthalmol Vis Sci. 1999; 40:1702–1709. [PubMed: 10393039]

Morrison JC, Moore CG, Deppmeier LM, Gold BG, Meshul CK, Johnson EC. A rat model of chronic pressure-induced optic nerve damage. Exp Eye Res. 1997; 64:85–96. [PubMed: 9093024]

Neufeld AH, Sawada A, Becker B. Inhibition of nitric-oxide synthase 2 by aminoguanidine provides neuroprotection of retinal ganglion cells in a rat model of chronic glaucoma. Proc Natl Acad Sci U S A. 1999; 96:9944–9948. [PubMed: 10449799]

Nguyen JV, Soto I, Kim KY, Bushong EA, Oglesby E, Valiente-Soriano FJ, Yang Z, Davis CH, Bedont JL, Son JL, Wei JO, Buchman VL, Zack DJ, Vidal-Sanz M, Ellisman MH, Marsh-Armstrong N. Myelination transition zone astrocytes are constitutively phagocytic and have synuclein dependent reactivity in glaucoma. Proc Natl Acad Sci U S A. 2011; 108:1176–1181. [PubMed: 21199938]

Nissirios N, Chanis R, Johnson E, Morrison J, Cepurna WO, Jia L, Mittag T, Danias J. Comparison of anterior segment structures in two rat glaucoma models: an ultrasound biomicroscopic study. Invest Ophthalmol Vis Sci. 2008; 49:2478–2482. [PubMed: 18515586]

Ollivier FJ, Brooks DE, Kallberg ME, Sapp HL, Komaromy AM, Stevens GR, Dawson WW, Sherwood MB, Lambrou GN. Time-specific intraocular pressure curves in Rhesus macaques (Macaca mulatta) with laser-induced ocular hypertension. Vet Ophthalmol. 2004; 7:23–27. [PubMed: 14738503]

Onda E, Cioffi GA, Bacon DR, Van Buskirk EM. Microvasculature of the human optic nerve. Am J Ophthalmol. 1995; 120:92–102. [PubMed: 7611333]

Pang IH, Johnson EC, Jia L, Cepurna WO, Shepard AR, Hellberg MR, Clark AF, Morrison JC. Evaluation of inducible nitric oxide synthase in glaucomatous optic neuropathy and pressure-induced optic nerve damage. Invest Ophthalmol Vis Sci. 2005a; 46:1313–1321. [PubMed: 15790897]

Pang IH, Wang WH, Clark AF. Acute effects of glaucoma medications on rat intraocular pressure. Exp Eye Res. 2005b; 80:207–214. [PubMed: 15670799]

Park KH, Cozier F, Ong OC, Caprioli J. Induction of heat shock protein 72 protects retinal ganglion cells in a rat glaucoma model. Invest Ophthalmol Vis Sci. 2001; 42:1522–1530. [PubMed: 11381056]

Pease ME, Cone FE, Gelman S, Son JL, Quigley HA. Calibration of the TonoLab tonometer in mice with spontaneous or experimental glaucoma. Invest Ophthalmol Vis Sci. 2010; 52:858–864. [PubMed: 20720229]

Pease ME, Hammond JC, Quigley HA. Manometric calibration and comparison of TonoLab and TonoPen tonometers in rats with experimental glaucoma and in normal mice. J Glaucoma. 2006; 15:512–519. [PubMed: 17106364]

Pease ME, Zack DJ, Berlinicke C, Bloom K, Cone F, Wang Y, Klein RL, Hauswirth WW, Quigley HA. Effect of CNTF on retinal ganglion cell survival in experimental glaucoma. Invest Ophthalmol Vis Sci. 2009; 50:2194–2200. [PubMed: 19060281]

Prasanna G, Hulet C, Desai D, Krishnamoorthy RR, Narayan S, Brun AM, Suburo AM, Yorio T. Effect of elevated intraocular pressure on endothelin-1 in a rat model of glaucoma. Pharmacol Res. 2005; 51:41–50. [PubMed: 15519534]

Quigley HA, Addicks EM. Chronic experimental glaucoma in primates. I. Production of elevated intraocular pressure by anterior chamber injection of autologous ghost red blood cells. Invest Ophthalmol Vis Sci. 1980; 19:126–136. [PubMed: 6766124]

Quigley HA, Addicks EM. Regional differences in the structure of the lamina cribrosa and their relation to glaucomatous optic nerve damage. Arch Ophthalmol. 1981; 99:137–143. [PubMed: 7458737]

Quigley HA, Anderson DR. Distribution of axonal transport blockade by acute intraocular pressure elevation in the primate optic nerve head. Invest Ophthalmol Vis Sci. 1977; 16:640–644. [PubMed: 68942]

Rowland JM, Potter DE, Reiter RJ. Circadian rhythm in intraocular pressure: a rabbit model. Curr Eye Res. 1981; 1:169–173. [PubMed: 7297102]

Samsel PA, Kisiswa L, Erichsen JT, Cross SD, Morgan JE. A novel method for the induction of experimental glaucoma using magnetic microspheres. Invest Ophthalmol Vis Sci. 2010; 52:1671–1675. [PubMed: 20926815]

Sappington RM, Carlson BJ, Crish SD, Calkins DJ. The microbead occlusion model: a paradigm for induced ocular hypertension in rats and mice. Invest Ophthalmol Vis Sci. 2009; 51:207–216. [PubMed: 19850836]

Sawada A, Neufeld AH. Confirmation of the rat model of chronic, moderately elevated intraocular pressure. Exp Eye Res. 1999; 69:525–531. [PubMed: 10548472]

Schlamp CL, Li Y, Dietz JA, Janssen KT, Nickells RW. Progressive ganglion cell loss and optic nerve degeneration in DBA/2J mice is variable and asymmetric. BMC Neurosci. 2006; 7

Shareef SR, Garcia-Valenzuela E, Salierno A, Walsh J, Sharma SC. Chronic ocular hypertension following episcleral venous occlusion in rats [letter]. Exp Eye Res. 1995; 61:379–382. [PubMed: 7556500]

Sigal IA, Yang H, Roberts MD, Grimm JL, Burgoyne CF, Demirel S, Downs JC. IOP-induced lamina cribrosa deformation and scleral canal expansion: independent or related? Invest Ophthalmol Vis Sci. 2011; 52:9023–9032. [PubMed: 21989723]

Sugiyama K, Gu ZB, Kawase C, Yamamoto T, Kitazawa Y. Optic nerve and peripapillary choroidal microvasculature of the rat eye. Invest Ophthalmol Vis Sci. 1999; 40:3084–3090. [PubMed: 10586928]

Sun D, Lye-Barthel M, Masland RH, Jakobs TC. The morphology and spatial arrangement of astrocytes in the optic nerve head of the mouse. J Comp Neurol. 2009; 516:1–19. [PubMed: 19562764]

Taylor S, Calder CJ, Albon J, Erichsen JT, Boulton ME, Morgan JE. Involvement of the CD200 receptor complex in microglia activation in experimental glaucoma. Exp Eye Res. 2011; 92:338–343. [PubMed: 21296076]

Tehrani S, Johnson EC, Cepurna WO, Morrison JC. Astrocyte processes label for filamentous actin and reorient early within the optic nerve head in a rat glaucoma model. Invest Ophthalmol Vis Sci. 2014; 55:6945–6952. [PubMed: 25257054]

Tezel G, Yang X, Luo C, Cai J, Powell DW. An astrocyte-specific proteomic approach to inflammatory responses in experimental rat glaucoma. Invest Ophthalmol Vis Sci. 2012; 53:4220–4233. [PubMed: 22570341]

Valderrama CM, Li R, Liu JH. Direct effect of light on 24-h variation of aqueous humor protein concentration in Sprague-Dawley rats. Exp Eye Res. 2008; 87:487–491. [PubMed: 18822284]

Walsh, MM.; Yi, H.; Friedman, J.; Cho, KI.; Tserentsoodol, N.; McKinnon, S.; Searle, K.; Yeh, A.; Ferreira, PA. Experimental biology and medicine. Vol. 234. Maywood, N.J: 2009. Gene and protein expression pilot profiling and biomarkers in an experimental mouse model of hypertensive glaucoma; p. 918-930.

Wang WH, Millar JC, Pang IH, Wax MB, Clark AF. Noninvasive measurement of rodent intraocular pressure with a rebound tonometer. Invest Ophthalmol Vis Sci. 2005; 46:4617–4621. [PubMed: 16303957]

WoldeMussie E, Ruiz G, Wijono M, Wheeler LA. Neuroprotection of retinal ganglion cells by brimonidine in rats with laser-induced chronic ocular hypertension. Invest Ophthalmol Vis Sci. 2001; 42:2849–2855. [PubMed: 11687528]

Yang MH, Dibas A, Tyan YC. Changes in retinal aquaporin-9 (AQP9) expression in glaucoma. Biosci. Rep. 2013; 33

Highlights

Retrograde injection of hypertonic saline into aqueous humor outflow pathways produces sclerosis and increased outflow resistance, with development of increased intraocular pressure (IOP) several days following injection.

Detecting the extent and duration of IOP elevation requires thorough understanding of extrinsic (general anesthesia) and intrinsic factors (circadian variation) that may affect IOP. Even with this knowledge, IOP fluctuation should be expected, necessitating at least 3 pressure recordings a week to gain the best possible understanding of the IOP to which the optic nerve is exposed.

Correlation of IOP history to nerve damage should be performed using multiple analyses, including consideration of mean, peak, duration and fluctuation in IOP, as well as integral IOP, or area under the curve of IOP vs time. Consultation with a statistician is recommended, particularly when designing and analyzing neuroprotection studies.

Despite the challenges of exacting surgical skill and demanding attention to detail, hypertonic saline injection can be successfully learned with practice.

IOP elevation from hypertonic saline injection, as well as other methods that obstruct aqueous humor outflow, reproduce scleral stresses and strains that may affect axons in the optic nerve head and afford opportunities to understand cellular mechanisms of glaucomatous optic nerve damage.

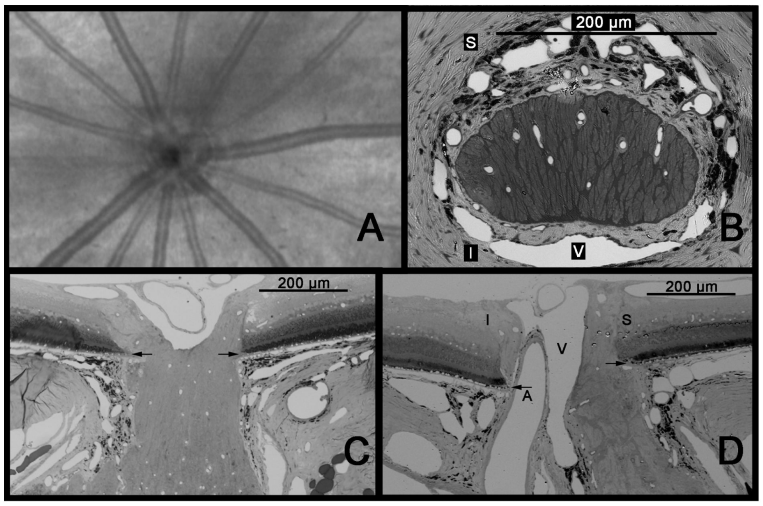

Figure 1.

Anatomy of the rat ONH. A. Anterior view of the rat fundus as seen by Optical Coherence Tomography (OCT). The ONH is dominated by spoke-like retinal arteries and veins that all but obscure the actual neural portion of the ONH. B. Cross-sectional view of the ONH at the level of the sclera. The nerve is horizontally oval and densely surrounded by vessels, including the central retinal vein (V), which is located inferiorly. The central retinal artery (not seen) lies inferior to the vein. C. Horizontal longitudinal section shows the optic nerve contacting the edge of Bruch's membrane at either extreme. D. A vertical longitudinal section shows that only the superior aspect of the nerve is in contact with the edge of Bruch's membrane, while inferiorly, the ONH is separated from Bruch's by the central retinal artery as well as the vein. Arrows = Bruch's membrane; S = superior; I = inferior; A = central retinal artery; V = central retinal vein. (A. Courtesy of R. Wang and Z. Zhi)

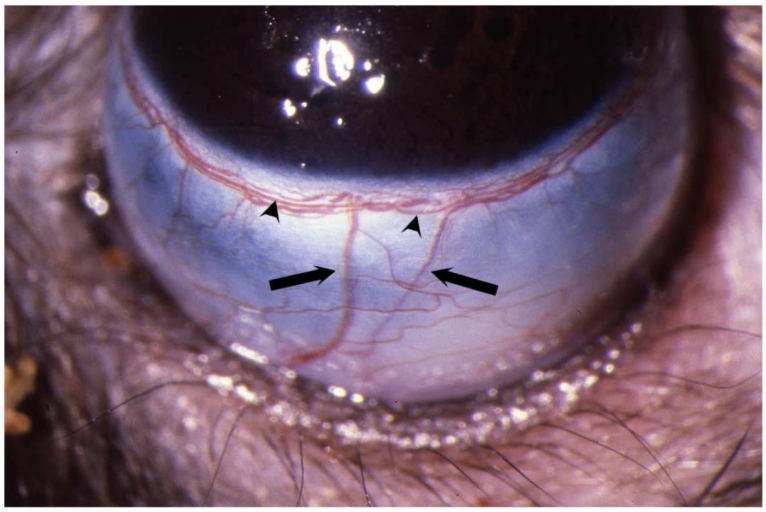

Figure 2.

External view of the rat limbus from the perspective of the operator, illustrating radial episcleral veins (arrows) that drain the limbal plexus, one of which would be injected with hypertonic saline. Limbal artery (arrowheads) within the plexus can be differentiated from veins as it is relatively straight, and does not branch.

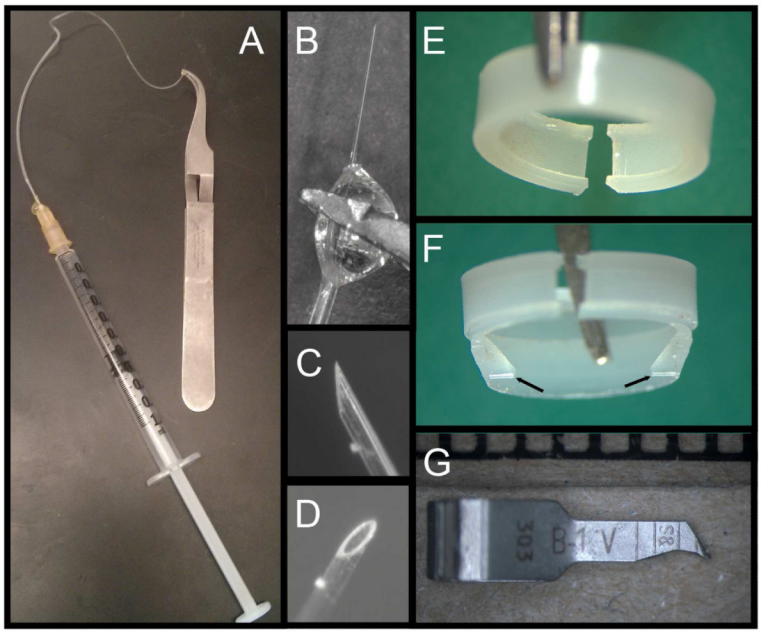

Figure 3.

Specialized equipment for hypertonic saline injection. A. The entire microneedle assembly with self-locking forceps. B. Detailed view of tubing:microneedle junction held at the glue joint by forceps, along with beveled needle tip (C and D). E. Standard plastic ring used to compress episcleral veins to confine injected saline to the limbus. F. Irregular ring cast to form internal projections (arrows) that apply focal pressure to constrict Schlemm's canal and limit circumferential flow of injected saline. G. Vascular microclip (viewed next to a millimeter scale), sharpened to constrict vessels not occluded by the ring.

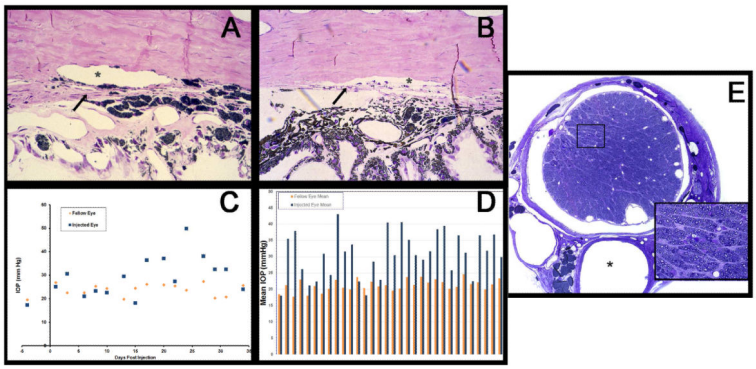

Figure 4.

Consequences of hypertonic saline injection. A. and B. Effect of hypertonic saline injection on anterior chamber angle. A. Schlemm's canal (asterisk) still appears patent but trabecular meshwork (arrow) is thickened and scarred, compared to normal, uninjected angle (B). C. IOP curves of experimental (injected) and fellow (uninjected) eyes in a single animal following episcleral vein injection measured by Tonolab. Onset of IOP elevation occurs several days following saline injection. IOP of uninjected, fellow eye demonstrates moderate variability in the low to mid-twenties. With the TonoPen, fellow eye readings tend to show less variability. D. IOP means over 35 days in a group of 32 animals, comparing injected eyes to fellow, uninjected eyes. E. Cross section through the myelinated optic nerve demonstrating typical injury pattern in an eye with partial injury (grade 2.4). Central retinal artery (asterisk) is seen inferiorly, indicating that the focus of axonal degeneration (outlined box and inset) is located in the superior portion of the optic nerve.

Author Manuscript

Author Manuscript

Author Manuscript

Table 1

Instruments for hypertonic saline injection

Fine tip jeweler's forceps Dumont #5SF Forceps Fine Science Tools 11252-00 (Foster City, CA)
Fine-tipped Vannas Capsulotomy Scissors Curved Storz E3387 Bausch & Lomb Surgical, Inc. (Rancho Cucamonga, CA)
Microneedle with attached, tapered tubing
Dumont Self-Closing #N7 Curved Forceps Fine Science Tools 11267-30 to hold microneedle
Hypertonic saline (1.5 – 2.0 M) filtered through a millipore filter into 1 cc syringe Plastic limbal ring
Fine vessel clamps, S&T Vascular Clamps Fine Science Tools 00396-01